Molecular Properties of p-(Dimethylamino)benzaldehyde Bound to Liver Alcohol Dehydrogenase: A Raman Spectroscopic Study†

Robert Callender,*,‡ Dehuai Chen,‡ Johan Lugtenburg,§ Charlotte Martin,∥ Kee Woo Rhee,‡ Donald Sloan,∥ Robert Vandersteen,§ and Kwok To Yue⊥

Physics and Chemistry Departments, City College of the City University of New York, New York, New York 10031, Physics Department, Emory University, Atlanta, Georgia 30322, and Chemistry Department, State University of Leiden, Leiden, The Netherlands

Received September 15, 1987; Revised Manuscript Received December 24, 1987

ABSTRACT: We have studied the binding nature of an aromatic aldehyde to the catalytic site of liver alcohol dehydrogenase from horse (LADH) using preresonance Raman spectroscopy. The compound p-(dimethylamino)benzaldehyde (DABA) is converted to the corresponding alcohol in the presence of nicotinamide adenine dinucleotide (NADH) and a catalytic amount of enzyme at neutral pH. A stable ternary complex of LADH/NADH/DABA can be formed if enzyme and coenzyme are in excess at high pH [Jagodzinski, P. W., Funk, G. F., & Peticolas, W. L. (1982) *Biochemistry 21*, 2193-2202]. We have obtained the preresonance Raman spectrum of bound DABA by subtracting the contribution of the binary complex of LADH/NADH from the spectrum of this stable ternary complex. In order to understand the normal mode patterns of DABA, four isotopically labeled DABA derivatives were synthesized and their Raman spectra, in solution and in the ternary complex, were measured. Three of these compounds contain substitutions in the functionally important aldehyde moiety: (i) In one such substitution, the aldehydic hydrogen atom was replaced by a deuterium; (ii) in another, this hydrogen atom was replaced by deuterium, and the aldehydic carbon atom was replaced by ^{13}C; and (iii) in the third derivative, only the carbon atom was replaced by ^{13}C. The fourth derivative has had the two hydrogen atoms at the 3- and 5-positions of the DABA ring replaced by deuterium atoms. We find that many of the spectral modes are fairly extended, involving both stretching and bending motions of the entire molecule, although a few modes are quite localized. We find that the normal mode structure of DABA changes considerably when it binds to LADH/NADH. As a model for the bound DABA, we have examined the zinc complexes of DABA (and all four isotopically labeled samples) in anhydrous diethyl ether and methylene chloride. A striking correspondence between the Raman spectra of the enzyme-bound DABA and DABA-Zn complexes in solution is found, which extends to all the isotopically labeled derivatives. This suggests that one of the major roles of LADH in the binding of DABA is to provide a divalent zinc ion to form a first-sphere Lewis acid complex. The data also suggest other interactions between enzyme-bound DABA with its protein surroundings and with the coenzyme NADH are quite minor. An estimate of the carbonyl bond character of bound DABA had been made on the basis of the response of Raman bands to isotopic labeling and on trends observed in spectra of DABA in solvents of various polarities. It is found to have a bond order between a single and double bond. We discuss a possible role of the zinc ion at the enzyme's active site and subsequently the mechanism of the enzymatic function of LADH in view of these results.

Horse liver alcohol dehydrogenase [EC 1.1.1.1 (LADH)[1]] catalyzes the interconversion of aldehydes and their corresponding alcohols with the oxidation/reduction of nicotinamide adenine dinucleotide coenzyme, NADH and NAD^+. It has been shown that the general catalytic behavior of LADH is described by the Theorell-Chance mechanism (Theorell & Chance, 1951) with a sequential order of coenzyme and substrate binding and an ordered release of products. X-ray crystallographic studies [reviewed in Eklund and Brändén (1986)] revealed that LADH contains two regions: a coenzyme-binding domain and a substrate-binding pocket situated in close proximity, so that the nicotinamide head is brought close to the aldehydic carbon of the substrate. This facilitates the transfer of a hydride ion from NADH to the bound aldehyde, or, in the reverse direction, the hydride transfer from the alcohol to NAD^+. At the apex of the substrate pocket lies a tetrahedrally coordinated Zn(II) cation. Three of its ligands are Cys-174, His-67, and Cys-46. The fourth ligand is a water molecule. An important issue concerns the role of zinc in substrate binding. Another crucial problem is the electronic nature of the bound substrate, which is, of course, key to understanding how the hydride transfer takes place in molecular terms.

It is not clear whether all substrates are bound directly to the active Zn(II) metal cation or whether a second-sphere

† This work was supported by Grant GM35183 from the National Institutes of Health, the Netherlands Foundation for Chemical Research (SON), and the Netherlands Organization for the Advancement of Pure Research (ZWO).

‡ Physics Department, City College of the City University of New York.

§ Chemistry Department, State University of Leiden.

∥ Chemistry Department, City College of the City University of New York.

⊥ Physics Department, Emory University.

[1] Abbreviations: DABA, p-(dimethylamino)benzaldehyde; DACA, p-(dimethylamino)cinnamaldehyde; DMF, dimethylformamide; LADH, liver alcohol dehydrogenase; NADH, reduced β-nicotinamide adenine dinucleotide; NAD^+, oxidized β-nicotinamide adenine dinucleotide; THF, tetrahydrofuran; ADPR, adenosine 5′-diphosphate ribose; AIBN, azobis(isobutyronitrile).

0006-2960/88/0427-3672$01.50/0

coordination occurs in some cases. X-ray crystallographic studies on ternary complexes with inhibitors and with the chromophoric substrate *p*-(dimethylamino)cinnamaldehyde (DACA) have strongly suggested a direct coordination of the substrate to the active-site zinc ion (Brändèn & Eklund, 1978, 1980; Eklund et al., 1981; Plapp et al., 1978; Cedergren-Zeppezauer et al., 1982). Further support comes from kinetic studies (Taniguchi et al., 1967) and studies of the pH dependence of LADH catalysis (Kvassman & Pettersson, 1978, 1980a,b). Dunn and his colleagues examined many aromatic substrates and performed extensive studies on the chromophoric substrate DACA (Dunn & Hutchison 1973; Dunn et al., 1975; Morris et al., 1980; Cedergren-Zeppezauer et al., 1982; Dahl & Dunn, 1984). They proposed that first-sphere coordination occurs between the substrate's carbonyl oxygen and the active-site zinc ion, mainly on the basis of X-ray crystallographic structures and on the large red shift in λ_{max} of DACA, which results when it binds to the enzyme and coenzyme complex. Such red shifts can be readily understood on the basis of the formation of a direct DACA–Zn complex. In fact, such red-shifted complexes can be readily formed with $ZnCl_2$ in organic solvents (Angelis et al., 1977; Jagodzinski et al., 1982). On the other hand, Sloan et al. (1975) have proposed that the metal ion remains coordinated to a water molecule (or hydroxyl ion) and that the substrate is hydrogen bonded to this water molecule on the basis of magnetic relaxation studies with cobalt-substituted LADH. Another NMR report (Drysdale & Hollis, 1980) and experiments concerning substitute effects in alcohol oxidation (Hardman et al., 1974; Blackmann & Hardman, 1975) also support a second-sphere interaction. Shore and co-workers suggested a covalent attachment of the alcoholic hydroxyl group to the basic form of a perturbed functional group of the enzyme rather than to the active-site zinc ion (Shore et al., 1974).

Raman spectroscopy is known for its abiliity to provide detailed information concerning the molecular properties of biologically interesting molecules. This is particularly important since structural probes, such as X-ray diffraction studies, cannot determine the nature of a molecule's electron distribution. Thus, key factors such as bonding properties and substrate oxidation state have rarely been quantitatively studied and are largely unknown. Recently, Peticolas and his coworkers (Jagodzinski & Peticolas, 1981; Jagodzinski et al., 1982) reported the Raman spectrum of the ternary complex of the aromatic chromophore *p*-(dimethylamino)benzaldehyde (DABA) with LADH and NADH. Previous kinetic studies had shown that DABA is converted to the corresponding alcohol in the presence of LADH and NADH around neutral pH (Dworschack & Plapp, 1977). However, a stable ternary complex can be formed around pH 9.6 with excess enzyme and coenzyme (Jagodzinski et al., 1982). The formation of the complex is readily detected since DABA's λ_{max} is considerably red shifted upon complex formation. The LADH/NADH/DABA Raman spectrum contains a substantial contribution from bound DABA due to some preresonance enhancement of DABA's Raman cross section. The λ_{max} of 380 nm for bound DABA is fairly close to the 488-nm laser excitation used in their work. Problems with DABA fluorescence precluded the use of lower wavelength excitation, which would have resonantly enhanced DABA's Raman cross section to the point of dominating the ternary complex spectrum. These investigators also reported the Raman spectra of DABA–Zn complexes in organic solvents. It was observed that the Raman spectra of DABA–Zn complexes are very similar to the spectrum of bound DABA.

In the present study, we have extended this Raman spectral analysis along several lines. First, we have been interested in applying difference Raman spectroscopy to obtain the Raman spectrum of a small ligand (coenzyme or substrate) when bound to a large protein (Yue et al., 1984; Chen et al., 1987) by subtracting the contribution of the protein from the complex spectrum. Differences of 1% can be reliably obtained. These techniques allow us to obtain the Raman spectrum of the bound DABA without the contribution of the enzyme and the coenzyme. These conditions permit a much better and more detailed comparison between the spectra of bound DABA and DABA–Zn complexes. Second, we have obtained the Raman spectra from a series of isotopically labeled DABA molecules in solution, in DABA–Zn complexes, and in DABA bound to LADH/NADH. Such data are required for any understanding of the spectroscopy of DABA and, thus, its molecular properties. While we do not have sufficient data to develop a molecular force field, the data do form a basis for a qualitative and semiquantitative assignment of the bands. Thus, the changes in molecular properties that take place when DABA binds to LADH/NADH can be assessed. We have also examined the Raman spectra of DABA in various solvents with different dielectric constants. The visible absorption band of DABA is due to a $\pi\pi^*$ transition. The excited state of DABA is believed to consist predominantly of a polar valence bond structure (see Discussion). Several polar resonance structures can contribute to the ground state, with the amount of contribution depending on the polarity of the media. Thus, the $\pi\pi^*$ transition is affected by polar media, and DABA's λ_{max} may be varied considerably depending on solvent polarity. At the same time, the bond orders of the ground state also change markedly, and this affects the frequencies of the observed Raman bands. The correlation between λ_{max} and changes in the spectra is very useful in interpreting the Raman data of the bound chromophore. We also show the existence of a stable ternary complex consisting of LADH, DABA, and an inactive coenzyme analogue, 1,4,5,6-tetrahydronicotinamide adenine dinucleotide (H_2NADH), near neutral pH. This ternary complex has absorption and Raman spectra identical with those of LADH/NADH/DABA.

Materials and Methods

Horse liver alcohol dehydrogenase (LADH) was purchased as a crystalline suspension in 10% ethanol from Boehringer Mannheim Co. (Indianapolis, IN) and stored at 4 °C until needed. Before use, the enzyme was prepared as described earlier (Chen et al., 1987). The specific activity was determined by the method of Dalziel (Dalziel, 1963). No preparation with specific activity less than that reported by Dalziel was used in these experiments. NADH was purchased from either Sigma Chemical Co. (grade III; St. Louis, MO) or from Boehringer Mannheim Co. (100%) and used without further purification. Concentrations of LADH and NADH were determined spectroscopically by using $\epsilon_{280} = 3.57 \times 10^4$ M^{-1} cm^{-1} for LADH and $\epsilon_{340} = 0.622 \times 10^4$ M^{-1} cm^{-1} and $\epsilon_{259} = 1.44 \times 10^4$ M^{-1} cm^{-1} for NADH. DABA was also purchased from Sigma and stored in the dark over a desiccant prior to use. Typically, the ternary complex of LADH/NADH/DABA was prepared by mixing a 1:2:0.67 molar ratio of LADH to NADH to DABA. Under these conditions, all DABA molecules are enzyme bound. The binary complex of LADH/NADH was prepared in a molar ratio of 1:2 LADH to NADH. All samples were maintained at 4 °C by a circulator/bath. Aqueous solutions of DABA were obtained by dissolving this substrate in 0.1 M pyrophosphate (pH 9.6) solution. $ZnCl_2$ was purchased from Mallinckrodt, Inc. (St.

Louis, MO). Anhydrous diethyl ether was obtained from either J. T. Baker Chemical Co. (Phillipsburg, NJ) or Fisher Scientific Co. (Fair Lawn, NJ). Methylene chloride was purchased from Fisher Scientific. Methylene chloride used in these preparations was determined to be dry enough upon arrival. Diethyl ether was dried with sodium before use. All nonaqueous solutions were prepared under an argon atmosphere. Other solvents were purchased from Sigma (spectrographic grade) and used without further purification. For the preparation of the DABA–Zn complexes, DABA and $ZnCl_2$ were dried in vacuo over phosphorus pentoxide and used immediately or stored in vacuo over phosphorus pentoxide. The DABA was dissolved in either anhydrous diethyl ether or methylene chloride to a concentration of 40 mM. A saturated solution of $ZnCl_2$ was prepared in either solvent. A 1:1 (v/v) mixture of both solutions was prepared. The DABA–Zn complex was considered to be formed by the criteria of the shift in λ_{max} from 327 nm, when free in solution, to 372 or 380 nm, when in complexation to zinc ion, in either diethyl ether or methylene chloride, respectively.

Raman spectra were measured with an optical multichannel analyzer (OMA) system consisting of a Triplemate spectrometer (Spex Industries, Metuchen, NJ), a Model 1420 reticon solid-state detector system with an intensified array of photodiodes, and a Model 1218 controller (EG&G, Princeton Applied Research, Princeton, NJ). Spectral lines were calibrated against known Raman lines of toluene. The detector was interfaced to an LSI-11 minicomputer (Digital Equipment Corp., Marlboro, MA) that was also used for analysis. Excitations were obtained by using either an argon ion laser (Model 165, Spectra Physics, Mountain View, CA) or a krypton ion laser (CR-2000, Coherent Radiation, Inc., Palo Alto, CA). Most spectra shown were measured by using the 488.0-nm line.

H_2NADH Preparation. 1,4,5,6-Tetrahydronicotinamide adenine dinucleotide (H_2NADH) was prepared from NADH by the methods of Biellman and Jung (1971) and Dunn et al. (1975). Binary and ternary enzyme complexes of this analogue were prepared in the same way as complexes with NADH.

Syntheses of the Isotopically Labeled DABA. (a) CDO-DABA Preparation. N,N-Dimethylaniline was subjected to a modified Vilsmeier–Haack reaction (de Groot et al., 1981). To a solution of 1.2 g (10 mmol) of *N,N*-dimethylaniline and 0.8 g (11 mmol) of DMF in 10 mL of ether was added 1 equiv (1.7 g) of $POCl_3$ at 0 °C with stirring. After this addition, the mixture was stirred for approximately 10 min. The iminium salt that precipitated was washed a few times with petroleum ether (40–60 °C). Thereafter, 20 mL of a 4 N NaOH solution was added at 0 °C. After extraction with ether, washing with brine, and drying with potassium carbonate, the crude aldehyde preparation was obtained. Purification by ether/SiO_2 chromatography yielded 1.0 g (67%) of DABA: ^{1}H NMR (100 MHz in $CDCl_3$) δ 3.04 (s, 2 × CH_3), 6.64 (d, 2 × ortho H, J_{AB} = 8 Hz), 7.66 (d, 2 × meta H), 9.64 (s, HCO).

Thereafter, 0.5 g (3.4 mmol) of this DABA solution was added to a mixture of 2.0 g (30 mmol) of KCN, 10 g of ative MnO_2, and 600 mg (10 mmol) of acetic acid in 100 mL of methanol, and the mixture was stirred at room temperature for 12 h (Pardoen et al., 1984). The solids were removed by filtration, the methanol was evaporated in vacuo, and the residue was partitioned between ether and water. The organic layer was washed with water, dried over $MgSO_4$, and concentrated to give 0.6 g (100%) of methyl *p*-(dimethylamino)benzoate: ^{1}H NMR δ 2.96 (s, 2 × CH_3), 3.80 (s, OCH_3), 6.60 (d, 2 × ortho H, J_{AB} = 8 Hz), 7.88 (d, 2 × meta H).

A solution of the methyl ester in dry ether was added dropwise to a stirred suspension of excess $LiAlD_4$ in dry ether at 0 °C. The mixture was stirred for 30 min and quenched by addition of water. The layers were separated, whereupon the aqueous layer was extracted with ether. This extract was washed with water followed by brine and then dried as before and concentrated. The residue containing the corresponding deuteriated alcohol was dissolved in toluene, and 10 equiv of silver carbonate was added to the solution (Fetizon et al., 1973). The mixture was refluxed until metallic silver precipitated. Then the solution was filtered over celite. Evaporation of the solvent yielded the crude CDO-DABA, which was purified by ether/SiO_2 chromatography. ^{1}H NMR showed the complete disappearance of the aldehyde signal.

(b) ^{13}CHO-DABA Preparation. N,N-Dimethylaniline (1.2 g, 10 mmol) was dissolved in 30 mL of THF (freshly distilled from $LiAlH_4$). One equivalent (2.5 g) of iodine was added together with a trace of AIBN at 0 °C. The solution was stirred for 2 h at 0 °C. Then ether was added, and the solution was washed subsequently with thiosulfate solution and water. After drying again with $MgSO_4$, the solvents were removed in vacuo. The crude mixture was purified by ether/SiO_2 chromatography to yield 1.4 g (70%) of *p*-iodo-*N,N*-dimethylaniline: ^{1}H NMR δ 2.92 (s, 2 × CH_3), 6.50 (d, 2 × ortho H, J_{AB} = 8 Hz), 7.40 (d, 2 × meta H).

The purified iodide (700 mg, 2.8 mmol) was dissolved in distilled DMF, and 500 mg (5.5 mmol) of Cu^{13}CN was added. (The labeled CuCN was prepared by adding 1 equiv of 90% enriched K^{13}CN to a heated suspension of 1 equiv of Cu^{I}Cl in water. After 1 h, the precipitated Cu^{13}CN was collected by filtration and dried.) The solution was refluxed for 4 h, after which time cooling water was added, and the mixture was extracted with ether. The organic layers were washed with water and brine and then dried over $MgSO_4$. The solvent was removed, and the residue was purified by ether/SiO_2 chromatography, yielding 300 mg (73%) of the pure (90% enriched ^{13}C) *p*-cyano-*N,N*-dimethylaniline: ^{1}H NMR δ 3.00 (s, 2 × CH_3), 6.56 (d, 2 × ortho H), 7.34 (dd, 2 × meta H, J_{AB} = 8 Hz, J^{13}_{C-H} = 5 Hz); IR (in KBr) 2215 cm^{-1} (C≡N stretch).

A total of 1.3 equiv of a 1 M solution of Dibal in hexane was added dropwise with a syringe to a solution containing 1 equiv of the nitrile in ether at −60 °C. The mixture was warmed to 0 °C, and after 1 h, a suspension of a 1:5 ratio of rater/silica gel was added and the mixture stirred at 0 °C for 1 h. After drying over K_2CO_3/$MgSO_4$, the solid material was separated and washed with dry ether. Evaporation of the solvent yielded the crude ^{13}CHO-DBA, which was purified by ether/SiO_2 chromatography (90% yield): ^{1}H NMR δ 3.04 (s, 2 × CH_3), 6.64 (d, 2 × ortho H) 7.66 (dd, 2 × meta H, J_{AB} = 8 Hz, J^{13}_{C-H} = 5 Hz), 9.62 (d, H^{13}CO, J^{13}_{C-H} = 166 Hz).

(c) ^{13}CDO-DABA Preparation. ^{13}CDO-DABA was prepared from ^{13}CHO-DABA by using the same method as described for the synthesis of CDO-DABA from CHO-DABA. In the ^{1}H NMR spectrum of ^{13}CDO-DABA the HCO signal at 9.62 ppm completely vanished.

(d) [3,5-$^2H_2$]DABA (2D DABA) Preparation. A mixture of *N,N*-dimethylaniline (2.0 mL), D_2O (7.0 mL), and $POCl_3$ (0.3 mL) was sealed in a glass tube and heated at 150 °C for 3 days (Sasaki & Sugiura, 1974). After cooling, the product was dissolved in 5% HCl and washed with ether. Then it was made alkaline with aqueous NH_4OH and saturated with NaCl. The liberated base was extracted with ether, and the organic

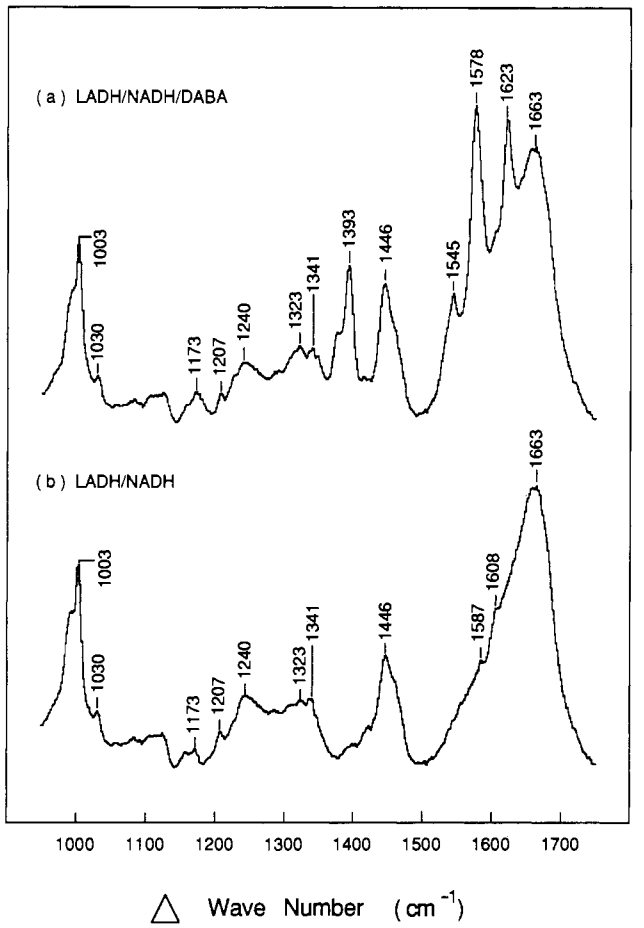

FIGURE 1: Raman spectra of (a) the ternary complex LADH/NADH/DABA with a molar ratio of 1:2:0.67 and (b) the binary complex of LADH/NADH with a molar ratio of 1:2. Both were in 0.1 M pyrophosphate buffer, pH 9.6 at 4 °C.

layer was dried over $MgSO_4$. The solvent was removed, and the residue was purified by ether/SiO_2 chromatography. ^1H NMR showed no ortho and para signals, only the meta H signal at 7.20 ppm. The deuteriated *N,N*-dimethylaniline was submitted to the same Vilsmeier–Haack reaction as described for CDO-DABA: ^1H NMR δ 2.98 (s, 2 × CH_3), 7.64 (s, 2 × meta H), 9.64 (s, HCO).

RESULTS

At pH 9.6, Peticolas and his co-workers (Jagodzinski & Peticolas, 1981; Jagodzinski et al., 1982) have shown that a stable ternary complex of LADH/NADH/DABA can be formed with an excess of enzyme and coenzyme. The λ_{max} of DABA in water at 352 nm shifts to 380 nm upon complex formation. Figure 1a shows the Raman spectrum of the ternary complex LADH/NADH/DABA at a molar ratio of 1:2.0:0.67 (LADH contains two active sites per molecule), using the 488-nm light for excitation. The spectrum agrees with previous results in Jagodzinski et al. (1982). Under the same conditions, the binary complex of LADH/NADH is shown in Figure 1b (Yue et al., 1984; Chen et al., 1987). Virtually all the peaks in the binary spectrum are protein bands of LADH. It is clear that bound DABA provides a very sizable contribution to the ternary complex spectrum. This is almost certainly due to preresonance enhancement of the Raman spectrum of DABA since the λ_{max} = 380 of bound DABA is close to the excitation wavelength of 488 nm.

The ternary complex spectrum (Figure 1a) was obtained with an enzyme concentration of 1.0 mM at pH 9.6. We have found in separate Raman and absorbance studies (data not shown) that the same spectra are obtained at pH 7.0 at these high enzyme concentrations of ca. 1.0 mM and the same 1:2.0:0.67 relative amounts of LADH, NADH, and DABA, respectively. In order to explore whether or not the ternary complex of these components occurs along the catalytic pathway, we performed similar measurements on complexes with H_2NADH, a derivative of NADH. The C5═C6 double bond of the nicotinamide ring in NADH is reduced to form this derivative. H_2NADH and NADH bind analogously to LADH (Dunn et al., 1975; Cedergren-Zeppezauer et al., 1982). H_2NADH forms stable ternary complexes with many carbonyl-containing substrates since it is unable to provide a hydride ion efficiently. Thus, the catalysis is blocked at this point. We obtained identical spectroscopic results from LADH/H_2NADH/DABA (at pH 7.0) and from LADH/NADH/DABA, strongly suggesting that the observed ternary complex mimics the catalytically important one.

The Raman spectrum of bound DABA alone can be obtained by subtracting the binary spectrum from the ternary spectrum. The results of this subtraction are shown in Figure 2b by using the protocol described by Chen et al. (1987). In that paper, it was shown how spectroscopic differences as small as 1% could be reliably obtained. Here, the subtraction is easier because of the much larger intensity of bound DABA, constituting some 30–50% of the complex signal (peak signals) for the most intense bands. It is possible that the difference spectrum of Figure 2b contains features due to changes in the LADH/NADH complex upon DABA binding in addition to the spectral features of bound DABA. This is, however, not the case. In the first place, X-ray crystallographic studies show no major conformation difference between binary and ternary complexes of LADH, including those of DACA (Cedergren-Zeppezauer et al., 1982), a closely related chromophoric substrate to DABA. Moreover, as will be evident below, most of the bands in Figure 2b respond to isotopic labeling of the bound DABA, and the spectra resemble very closely those of model zinc complexes.

We explored several model LADH/DABA systems. For exammple, the Raman spectrum of DABA in buffered (pH 9.6) water solution is shown in Figure 2a. There are substantial agreements between the two spectra, particularly in the 300–1000-cm^{-1} region. However, there are several rather important differences. Around 1400 cm^{-1}, there are two bands of considerable intensity for bound DABA in Figure 2b at 1378 and 1393 cm^{-1}, while there is only one prominent band at 1403 cm^{-1} in the spectrum of DABA in buffered solution in Figure 2a. Moreover, bands of similar intensity to the 1624- and 1578-cm^{-1} bands in the bound DABA spectrum are found in the DABA solution spectrum but at significantly shifted positions of 1644 and 1592 cm^{-1}, respectively. In addition, the solution band at 1644 cm^{-1} is considerably broader than the sharp 1624-cm^{-1} band in the bound spectrum. As we shall show below, the 1644-cm^{-1} band in the solution spectrum is probably two bands. Following previous work (Angelis et al., 1977; Jagodzinski et al., 1982), we formed Zn complexes of DABA by reacting $ZnCl_2$ with DABA in one of two solvents, methylene chloride or diethyl ether. DABA's λ_{max} = 337 nm in methylene chloride shifts to 380 nm upon formation of the complex, and similarly DABA's λ_{max} = 327 nm in diethyl ether shifts to 372 nm when coordination occurs (Jagodzinski et al., 1982; our data, not shown). The DABA–Zn complex λ_{max} values are much closer to that found for bound DABA and are, therefore, acceptable models. We found that the DABA–Zn complex yielded almost the same Raman spectrum for either solvent (see below). Figure 2c shows the spectrum

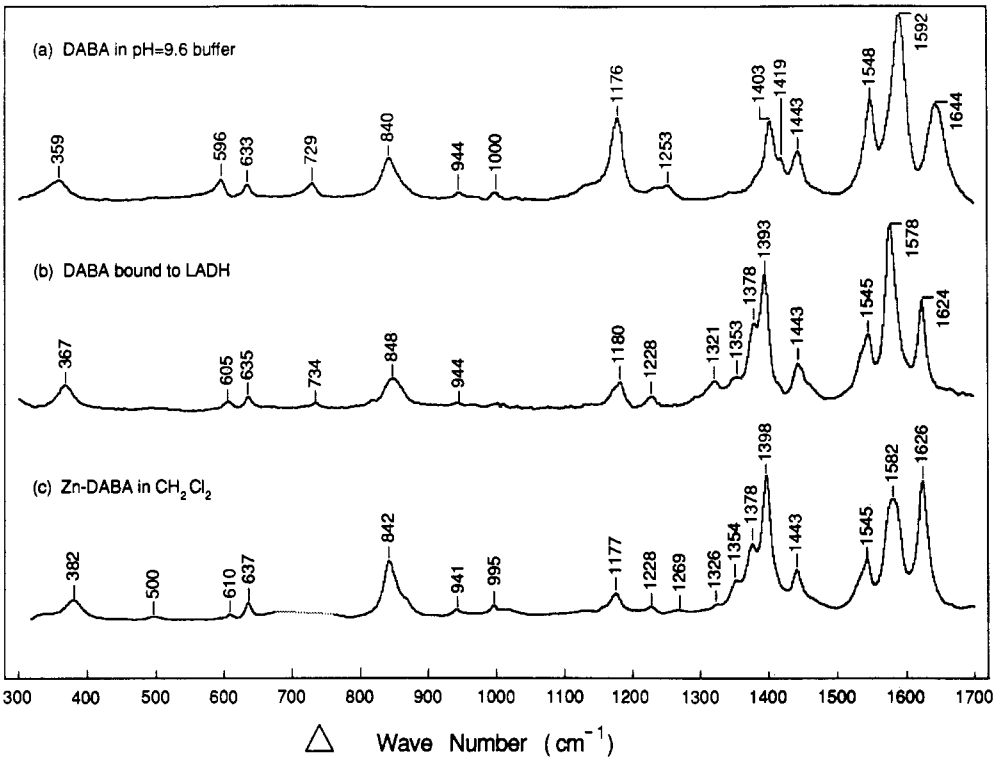

FIGURE 2: Raman spectra of (a) DABA (4.6 mM) in 0.1 pyrophosphate buffer, pH 9.6, (b) bound DABA calculated by taking the difference of the data in Figure 1, and (c) DABA–Zn complexed in methylene chloride (the data between 650 and 750 cm^{-1} are not plotted due to intensive solvent bands). All were 4 °C.

of the DABA–Zn complex in methylene chloride. The close correspondence between the DABA–Zn complex spectrum and the bound DABA spectrum of Figure 2b is remarkable, although not perfect. The most significant difference is between the intensity of the 1582-cm^{-1} band (Figure 2c) in the Zn complex spectrum and the relatively stronger (but narrower) 1578-cm^{-1} band of the enzyme-bound DABA (Figure 2b). DABA–Zn complex formed in diethyl ether (see below) yields a sharper and stronger 1582-cm^{-1} band. It is thus very likely that the observed 1582-cm^{-1} band in the Zn complex spectrum (and by comparison the 1578-cm^{-1} bound DABA band) consists of two degenerate or nearly degenerate modes that are somewhat solvent dependent.

It is important to take care in choosing the proper excitation wavelength for these Raman measurements. We have performed some preliminary measurements concerning the excitation wavelength dependence of the Raman spectra of these DABA–Zn complexes in the wavelength range between 457.9 and 514.5 nm. While the peak positions are not changed, significant relative intensity changes are found for the two highest frequency peaks (data not shown). As the excitation wavelength becomes shorter, the intensity of the highest frequency peak (1626 cm^{-1} in DABA–Zn in methylene chloride) increases, whereas that of the second highest frequency peak (1582 cm^{-1} in DABA–Zn in methylene chloride) decreases, relative to the other peaks. This is not unexpected from resonance or preresonance enhanced Raman spectra, since the normal modes of the various observed bands may couple differently to the electronic excited states of the molecule. This can give rise to different dependencies of Raman cross sections on the excitation wavelength. In theories of resonantly enhanced Raman cross sections, a most important parameter is the energy difference between the molecular absorption λ_{max} and the excitation wavelength. The best comparison between the enhanced spectrum of a chromophore and its model is one that keeps this difference constant. In our case, the λ_{max} value of the DABA–Zn complex in methylene chloride is identical with that of bound DABA. Therefore, all our measurements reported here were performed by using the same excitation wavelength, 488.0 nm.

In order to compare in detail the spectra obtained from the Zn complexes and bound DABA and to understand the normal mode pattern of DABA, we have obtained the Raman spectra from four isotopically labeled DABA derivatives. As described previously, three of these compounds have substitutions in the functionally important aldehyde moiety: (i) The aldehyde hydrogen has been replaced by a deuterium (called CDO in the graphs); (ii) the hydrogen atom has been replaced by a deuterium and the carbon atom replaced by ^{13}C (called ^{13}CDO); and (iii) the carbon atom has been replaced by ^{13}C (called ^{13}CHO). The fourth derivative, called 2D, has the two hydrogen atoms at the 3,5 carbon positions of DABA's ring replaced by deuterium atoms. Parts b–e of Figure 3 show the Raman spectra of these four samples, CDO, ^{13}CDO, ^{13}CHO, and 2D, respectively, in buffered solutions from 1000 to 1700 cm^{-1}. Figure 3a includes the Raman spectrum of unlabeled DABA (called CHO) in this range for comparison. The corresponding Raman spectra of bound DABA, and DABA–Zn complexes—in the same order of CHO, CDO, ^{13}CDO, ^{13}CHO, and 2D—are shown in Figures 4 and 5, respectively. Because of the low solubility of $ZnCl_2$ in methylene chloride, the Zn complex solution contains a small amount of free DABA in methylene chloride (less than 10%). In Figure 5, this contribution of free DABA to the spectrum as well as solvent bands has been subtracted.

The spectral changes in the 1000–1700-cm^{-1} region resulting from the isotopic labeling are dramatic and complex. It is clear that there are major differences between bound DABA and free DABA in buffered solutions (compare Figures 3 and 4) when the variously labeled derivatives are compared. This indicates that the force fields of DABA are very different in the two environments. On the other hand, the similarities

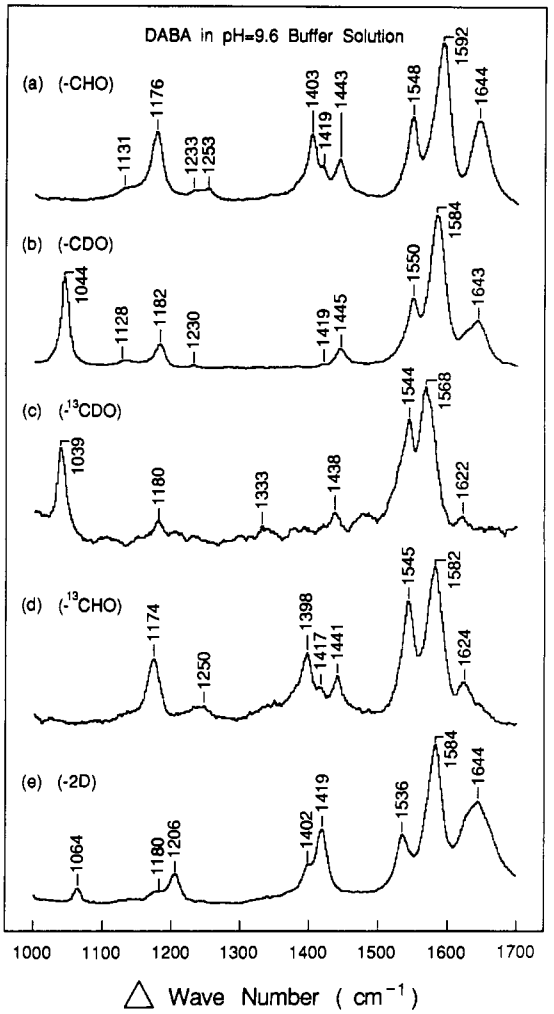

FIGURE 3: Raman spectra of (a) DABA (4.6 mM), (b) DABA (CDO) (7.3 mM), (c) DABA (^{13}CDO) (2.2 mM), (d) DABA (^{13}CHO) (4.3 mM), and (e) DABA (2D) (2.5 mM). All were in 0.1 pyrophosphate buffer, pH 9.6 at 4 °C.

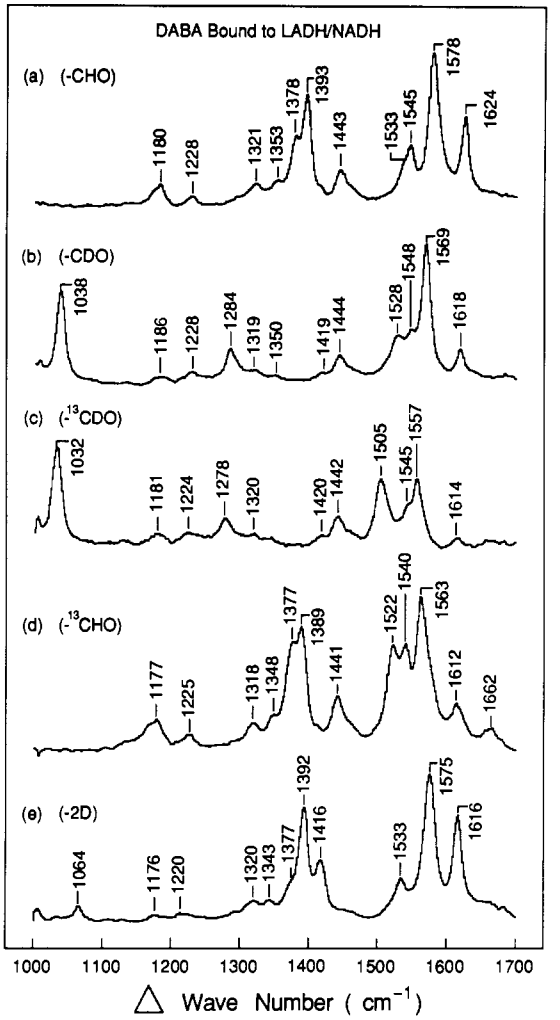

FIGURE 4: Raman spectra of bound (a) DABA, (b) DABA (CDO), (c) DABA (^{13}CDO), (d) DABA (^{13}CHO), and (e) DABA (2D). The molar concentrations are as in Figure 1, and the difference spectra are calculated as in Figure 2. All were in 0.1 pyrophosphate buffer, pH 9.6 at 4 °C.

between the spectra of all corresponding samples of bound DABA and DABA–Zn complex are striking (compare Figures 4 and 5). The DABA–Zn complexes are clearly excellent model systems that mimic the molecular properties of DABA bound to LADH.

Assignments of Peaks. We expect most of the normal modes of DABA to be quite delocalized because of the highly conjugated nature of the molecule. This general expectation is borne out by the isotopic data, where specific substitutions very often have substantial effects on many bands. The Raman spectrum of bound DABA in the 1000–1700-cm^{-1} range can be divided into two regions: one from 1500 to 1700 cm^{-1} and one from 1250 to 1500 cm^{-1}.

1500–1700-cm^{-1} Region. An important assignment concerns the frequency of the carbonyl (C=O) stretching since this is a marker for the bond order of this moiety. An isolated C=O bond, with a high degree of essential double-bond character, is expected to have a frequency at ca. 1700 cm^{-1}, while a C—O single-bond stretch might lie at ca. 1400 cm^{-1} [see Hertzberg (1950)]. As shown in Figure 6, we explored DABA's bond order and bond-order changes by plotting the Raman spectra of DABA in various solvents. The data are arranged by increasing λ_{max} (bottom to top in Figure 6) and range from values of 327 nm for DABA dissolved in diethyl ether to 372 nm for DABA–Zn complex in diethyl ether. The $\pi\pi^*$ electronic transition of DABA is red shifted in polar media essentially because the polar character of the excited state is stabilized (Angelis et al., 1977; Dahl & Dunn, 1984; see below). Concomitant with this, a greater mixture of several polar resonance structures, which have C–O character (see below), are brought into the ground state. Thus, the carbonyl bond becomes relatively lower in electron density and the amino group becomes relatively higher. We should observe a correlation between decreasing carbonyl frequency with increasing λ_{max}. This behavior is typical of such π electron systems [see, e.g., Carey and Storer (1984)].

The 1695-cm^{-1} band in the DABA/diethyl ether spectrum (Figure 6f) is almost an isolated pure C=O carbonyl stretch. This has been verified by Jagodzinski et al. (1982), who showed that this band shifts downward 40 cm^{-1} upon ^{16}O → ^{18}O substitution. A simple reduced mass calculation for an isolated C=O molecule predicts the same amount of downward shift. As λ_{max} increases, this band clearly shifts down in frequency, consistent with the concept of introducing more C–O character into the ground state. (It is also clear that there are two bands in this region, both of which are shifting toward lower frequency with increasing λ_{max}; both have substantial C=O character as seen below.) The DABA/water band at 1644 cm^{-1} still contains a great deal of C=O character. This can be demonstrated by its 20-cm^{-1} shift to 1624 cm^{-1} in the ^{13}CHO data of Figure 3d. A simple reduced mass calculation of an isolated C=O vibration at 1644 cm^{-1} yields a 36-cm^{-1} shift upon ^{12}C → ^{13}C substitution. Clearly, however, this

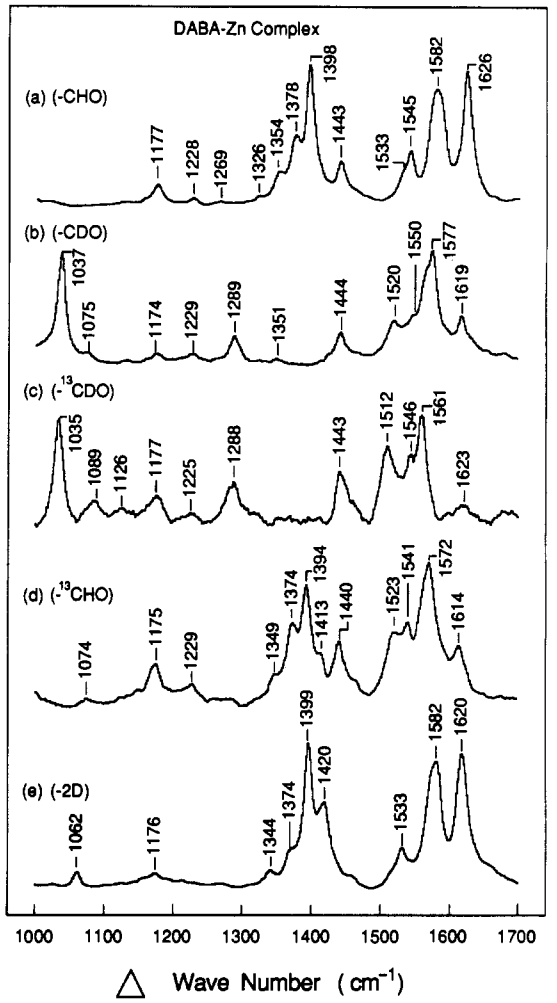

FIGURE 5: Raman spectra of DABA–Zn complexed (a) DABA, (b) DABA (CDO), (c) DABA (^{13}CDO), (d) DABA (^{13}CHO), and (e) DABA (2D). All were in methylene chloride at 4 °C and 20 mM concentration.

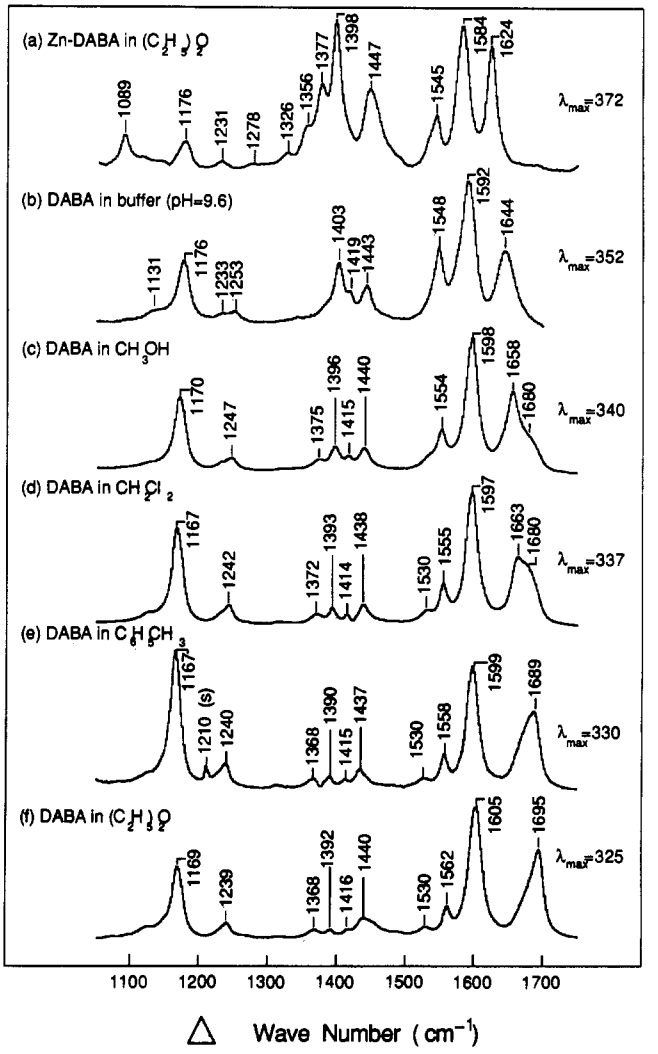

FIGURE 6: Raman spectra of DABA in different solvents: (a) DABA–Zn complexed (10 mM) in diethyl ether; (b) DABA (4.6 mM) in 0.1 pyrophosphate buffer, pH 9.6; (c) DABA (100 mM) in methyl alcohol; (d) DABA (100 mM) in methylene chloride; (e) DABA (100 mM) in toluene; (f) DABA (100 mM) in diethyl ether. All were at 4 °C.

normal mode also contains significant contributions from other internal coordinates. When the DABA–Zn complex is formed (Figure 6a), the λ_{max} is further red shifted, and the highest observed mode is lowered further to 1624 cm^{-1}. The 1624-cm^{-1} mode of the DABA–Zn complex apparently contains a still smaller C=O contribution, as judged from its 12-cm^{-1} shift upon $^{12}C \rightarrow {}^{13}C$ substitution (compare parts a and d of Figure 5) or its 8-cm^{-1} downward shift upon $^{16}O \rightarrow {}^{18}O$ substitution (Jagodzinski et al., 1982). In this regard, the 1584-cm^{-1} band in the DABA–Zn complex data has significant C=O character, as determined from its 10-cm^{-1} downward shift upon ^{13}C substitution (again compare parts a and d of Figure 5) and a 5-cm^{-1} shift upon ^{18}O substitution (Jagodzinski et al., 1982). The analogous mode for the enzyme-bound DABA data at 1578 cm^{-1} (Figure 4) shifts even further downward (15 cm^{-1}) to 1563 cm^{-1} upon ^{13}C substitution.

Qualitatively, this spectral behavior can be readily understood. So long as the C=O bond retains a high degree of essential double-bond character and is, therefore, the highest frequency mode for this molecule, there is very little mixing of this internal coordinate with other coordinates. When the frequency of this mode approaches the frequency of other internal coordinates, i.e., C=C stretching motion, then mode–mode mixing becomes more pronounced, and the mode takes on a more delocalized character. This is, of course, a two-way street. Other modes take on substantial C=O character when the C=O frequency becomes comparable. This is demonstrated by comparing the ^{13}C-substituted derivatives in either the bound spectrum (Figure 4d) of the DABA–Zn complex spectrum (Figure 5d) with the respective unsubstituted spectra (Figures 4a and 5a). All the bands in the 1500–1700-cm^{-1} region appear to show some sensitivity to ^{13}C labeling, with a number of very pronounced changes. Conversely, while there is some effect on the DABA/water spectrum upon ^{13}C labeling, it is not nearly as pronounced (Figure 3). This is consistent with a higher C=O and a more isolated carbonyl mode frequency for DABA in water.

This qualitative analysis suggests that the bond order of the carbonyl moiety of DABA is diminished upon zinc complexation (or bonding to the active site of LADH since the changes upon isotopic substitution are so similar) compared to that of, for example, DABA/water. However, the bond order must still be substantially larger than an essential single bond. We would suggest that the characteristic frequency of bound DABA's carbonyl moiety is within the 1550–1600-cm^{-1} range, judging from the trends defined in Figure 6 and the rather large effects on the bands in the 1500–1700-cm^{-1} region upon ^{13}C labeling. This value is about halfway between the aforementioned 1400-cm^{-1} frequency we have estimated for a carbonyl single bond and the 1700 cm^{-1} characteristic of a double bond. A detailed normal mode analysis would provide

a more quantitative picture of the bond order. However, such a presentation is premature at the present time. Data from a larger number of isotopic derivatives than we present here would be required to calculate an accurate force field due to the high degree of delocalization of most of DABA's modes.

All the observed modes in the 1500–1700-cm^{-1} range in the bound DABA spectrum (Figure 4a), and likewise the DABA–Zn complex spectra (Figure 5a), are affected by most of the isotopic labels. For example, the strong 1578-cm^{-1} band in the bound spectrum (Figure 4a) appears to shift to 1569 cm^{-1} upon CDO labeling and to 1663 cm^{-1} upon ^{13}CHO labeling. This band probably consists of two nearly degenerate modes, as can be seen from a comparison of the DABA–Zn complex spectra taken for Zn complexes in methylene chloride (Figure 5a) and in diethyl ether (Figure 6a). The peak in diethyl ether is sharper and relatively stronger, suggesting that the two modes have somewhat different solvent dependencies. That there appear to be two nearly degenerate modes may rationalize why the 1578-cm^{-1} band appears to shift to 1557 cm^{-1} in the enzyme-bound DABA data for the ^{13}CDO derivative (Figure 4c) but with much diminished relative intensity. The near degeneracy of the two modes may be lifted by ^{13}CDO substitution. The 1545-cm^{-1} band shows a 5-cm^{-1} downward shift upon ^{13}CHO substitution, suggesting some carbonyl contribution, and an apparent 13-cm^{-1} downward shift to 1533 cm^{-1} upon 2D substitution. The rather large effects on the 1624- and 1545-cm^{-1} bands and the smaller effect on the 1578-cm^{-1} band upon 2D substitution suggest that all these bands contain some ring hydrogen (in plane) bending contributions. This, combined with the effects of ^{13}CHO substitution, shows the extended nature of these modes and a mixed stretch-bend character.

1250–1500 cm^{-1} Region. This region contains peaks that are mostly due to bending motions. The data of Figure 6 suggest that the band positions in this region are relatively insensitive to different solvents and λ_{max}. The band intensities relative to those in the 1500–1700-cm^{-1} region, however, increase as the λ_{max} of the chromophore is red shifted. These are evidence that the normal mode character of these peaks does not change much as λ_{max} changes. For example, the 1393 cm^{-1} of DABA in methylene chloride disappears just as the 1393-cm^{-1} peak in the bound spectrum disappears upon deuteriation of the aldehyde hydrogen in CDO and ^{13}CDO samples (see below). The 1438-cm^{-1} DABA/CH_2Cl_2 peak also behaves the same way as the 1443-cm^{-1} peak in the bound data upon isotopic substitution (see below).

The isotopic substitutions have a dramatic effect on the bound DABA spectrum in the 1250–1500-cm^{-1} region (Figure 4a, and similarly on the Zn complex data of Figure 5a), and we present these changes here. Our presentation also applies to the DABA/water spectrum (Figure 5a) as there is a great deal of similarity. As mentioned above, unlike the 1500–1700-cm^{-1} modes, which contain significant stretch character, e.g., C=C, C=O, etc., the bending character of the 1250–1500-cm^{-1} modes is apparently relatively unaffected by π electron delocalization.

The only effect on the 1443-cm^{-1} band in the enzyme-bound DABA samples (Figure 4) by isotopic substitution is its shift (−27 cm^{-1}) to 1416 cm^{-1} for the 2D substitution. This mode can be assigned to bending motions of the ring hydrogens of DABA on the basis of this shift. The 1393-cm^{-1} mode shifts to 1038 cm^{-1} in the CDO data and to 1032 cm^{-1} in the ^{13}CDO data. This mode is almost purely due to carbonyl hydrogen bending. A simple reduced mass calculation on an isolated hydrogen-bending mode shows a $2^{1/2}$ decrease when the hydrogen is replaced by a deuterium. Thus, a "pure" mode at 1393 cm^{-1} would be predicted to shift to 985 cm^{-1}, very close to the observed shift. The 4–5-cm^{-1} shift in this mode upon ^{13}C substitution suggests a small, but significant, contribution from carbonyl carbon motion. The 1378-cm^{-1} band disappears upon deuteriation of the carbonyl group containing both ^{12}C and ^{13}C, and new bands appears at 1284 and 1278 cm^{-1}, respectively. This apparent shift of 94 cm^{-1} is quite large. Its intensity appears much reduced in the 2D data. It seems reasonable to assign this band preliminarily to hydrogen bending of both aldehyde hydrogen and ring hydrogens. However, the 6-cm^{-1} downward shift of the 1284-cm^{-1} mode in the CDO data to 1278 cm^{-1} in the ^{13}CDO data suggests some contribution from motion of the carbonyl carbon. The two smaller peaks at 1353 and 1321 cm^{-1} are not very sensitive to isotopic substitution.

Region below 1250 cm^{-1}. These lower frequency bands are changed very little when DABA binds to LADH, as is shown in Figure 3. Correspondingly, they are not particularly helpful in determining the changes in DABA's molecular properties when it binds. We present the behavior of these bands to isotopic substitution briefly.

The two peaks at ca. 1180 and 1228 cm^{-1} in the bound DABA spectrum (Figure 4a) are essentially independent of any isotopic substitution and are probably due to the ring skeleton stretching. It is interesting to note that, in the solution spectrum only (Figure 3), the two corresponding peaks are drastically changed in the 2D sample, indicating that they contain a significant amount of ring hydrogen bending motion in this case. The peak at 848 cm^{-1} in the bound spectrum (Figure 2b) consists of at least two modes since it is split into two peaks at 845 and 820 cm^{-1} in the 2D substitution. It is also significantly downshifted in all three aldehyde-substituted samples, CDO (to 815 cm^{-1}), ^{13}CDO (to 806 cm^{-1}), and ^{13}C-HO (to 838 cm^{-1}). Similar changes on substituted samples are observed for both the solution and the zinc complex spectra (all data not shown). The two peaks at 607 and 635 cm^{-1} in the bound spectrum (Figure 2b) are insensitive to the aldehyde's carbon or hydrogen substitution but downshifted by about 10 cm^{-1} in the 2D sample (data not shown). Again, similar behavior is observed for the solution and zinc complex spectra as a result of the isotopic labeling. It is interesting to note that the relative intensity patterns of these two peaks in the spectrum in bound DABA agrees with those of the zinc complex, but it is the opposite of that observed in the solution spectrum (compare parts a–c of Figure 2). The broad peak at 368 cm^{-1} in the enzyme-bound spectrum of DABA is relatively insensitive to our isotopic substitutions, a feature also shared by the solution and zinc complex DABA samples. It is interesting to note that this peak in the bound DABA spectrum is closer to that of this reactant in solution (at 360 cm^{-1}) than to that of DABA in the zinc complex (at 382 cm^{-1}).

Discussion

The involvement of the catalytic zinc ion as a Lewis acid in the catalytic behavior of LADH has been proposed by many investigators (Theorell & McKinley-McKee, 1961; Creighton & Sigman, 1971; Dunn & Hutchison, 1973; Dunn et al., 1975; Angelis et al., 1977; Jagodzinski et al., 1982). Direct coordination between the catalytic zinc and the carbonyl oxygen of the substrate has been suggested by many of these authors. For example, Dunn and his co-workers studied the aromatic substrate, DACA, using UV–visible absorption techniques. They concluded that the red shift due to ternary complex formation of this substrate with LADH/NADH is indicative of zinc ion acting as a Lewis acid. Jagodzinski et al. (1982)

correctly pointed out that there can be other reasons for this red shift. These authors reported Raman studies, which are more sensitive to detailed bonding changes than UV–visible absorption spectroscopy, on the ternary complex with DABA, and they concluded (correctly) that zinc complexes of DABA are good models for understanding the binding properties of DABA to LADH. DABA, however, is defined by a fairly complicated and rich Raman spectrum (see Results). The effect of isotopic substitutions on the Raman spectrum of DABA has permitted a more quantitative understanding of the observed bands and, thus, a much better demonstration of how accurate the DABA–Zn(II) complexes serve as a model for the bound chromophore. Moreover, we can begin to understand the electronic properties of the bound substrate with such data since Raman bands are sensitive to bond orders.

There are two central conclusions derived from our results. First, the character of DABA's modes, particularly in the 1500–1700-cm^{-1} region, changes dramatically when DABA binds to LADH to form the LADH/NADH/DABA complex. While DABA in water and in situ (at LADH's active site) yield Raman spectra that are, superficially, quite similar (Figure 2), the response of these modes to isotopic labeling is dramatically different. A rather major change in the force field describing the normal modes of DABA has occurred upon binding. Second, our results show an extremely close (although not identical) correspondence between the spectrum of bound DABA and that of DABA in zinc complex. The correspondence is especially striking with the isotopically substituted samples, excluding the possibility of accidental similarity between bound DABA and DABA in zinc ion complex. The success of the zinc-complex model essentially eliminates all but a direct ligation between LADH's active site Zn^{2+} and DABA. In particular, the possibility of a second-sphere interaction of catalytic zinc and this substrate is not possible. Moreover, keeping in mind that many of the bound DABA and DABA–Zn complex modes are highly delocalized, it is probable that additional specific polar interactions between DABA and its protein environment, apart from the ligation of DABA with the Zn^{2+} cation, would give rise to significant effects on the Raman spectrum of the bound DABA. There is no evidence for any such interactions since the DABA–Zn models yield Raman spectra so close to those of bound DABA. Thus, the Zn–DABA complex in a hydrophobic solvent can only be thought of as a good approximation of the enzyme-bound DABA.

These results are consistent with previous studies. X-ray crystallographic studies (Cedergren-Zeppezauer et al., 1982) have been performed on ternary complexes of LADH/H_2NADH with the aromatic substrate DACA to 2.9 Å. Their results indicate a direct coordination between the aldehyde oxygen of DACA and the Zn^{2+} cation of LADH. DACA was found to lie in an otherwise hydrophobic pocket. Interestingly, the aldehydic carbon of DACA was found to be 4 Å from the C4 atom of H_2NADH, an orientation where direct hydride transfer cannot take place. Thus, some repositioning of substrate and coenzyme toward each other is necessary for this direct hydride transfer to occur (Cedergren-Zeppezauer et al., 1982). In addition, recent rapid scanning stopped-flow studies by Dunn and his co-workers (MacGibbon et al., 1987) concerning the binding of 3-hydroxy-4-nitrobenzyl and other chromophoric substrates to LADH suggested that the active site of LADH could be divided into two subsites: a highly polar, electropositive subsite in the vicinity of the active-site zinc and a rather nonpolar region. They and others (Cedergren-Zeppezauer et al., 1982; Eklund et al., 1982) have speculated that the polar subsite promotes the hydride transfer between NADH and substrate while the nonpolar region acts as a binding site for the hydrocarbon-like side chains of LADH substrates.

As mentioned under Results, our data suggest that the carbonyl double-bond character lies halfway between a single and double bond when DABA binds to LADH/NADH as compared to DABA in solution. It is possible to consider a number of resonance structures to describe the electronic properties of the electronic ground state of DABA. A few of these are

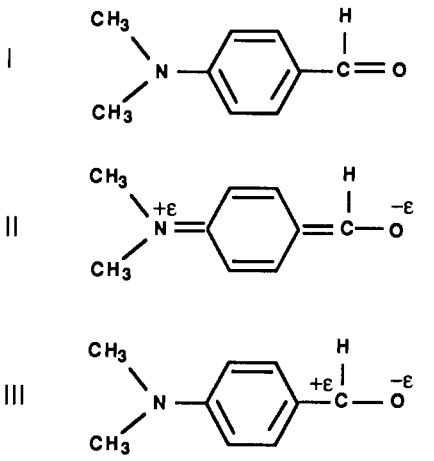

Structure I is characteristic of DABA's ground state when DABA is not complexed. Structures II and III are more characteristic of DABA's π electron excited states. The polar structures can readily form a charged pair complex between the partial negative charge on the carbonyl oxygen and the active-site Zn^{2+}. The partial positive charge induced is distributed throughout the rest of the molecule. Thus, the ligation of DABA to LADH presumably increases the proportion of these charged (polar) structures in the ground state, and this results in the observed much reduced carbonyl bond order found in bound DABA. Structure III is particularly favorable for hydride transfer compared to structure II. While DABA is readily converted to the corresponding alcohol, it is known that DABA is a rather poor substrate (Dworschack & Plapp, 1977) of LADH. A partial reason for this may be that little of the positive charge induced when DABA complexes with the active-site cation resides on the C1 position, relative to a nonaromatic substrate. Thus, hydride transfer from NADH to DABA's C1-position is relatively less favorable. This is depicted in Scheme I. In the aldehydes of primary alcohols, the electropositive nature of the zinc ion at the active site would create a much higher degree of charge separation between the carbon and oxygen of the aldehyde moiety. In these more physiological molecules, there is no energetically favorable way of creating extended resonance structures that would effectively remove partial positive charge from C1 as there is for DABA.

Clearly, the results of this study show that Raman spectroscopy can contribute significantly in determining the molecular properties of certain enzyme-bound substrates. With measurements of a somewhat larger number of isotopically labeled DABA derivatives than presented here, it seems feasible to derive a force field and bond orders of this substrate by fitting the observed differences in the Raman spectrum of the various labeled compounds in normal mode calculations. This can be done for DABA in solution and at the active site. Moreover, it may be possible to perform similar experiments on other chromophoric substrates that are, for example, better substrates of LADH than DABA. Comparison of different

Scheme I

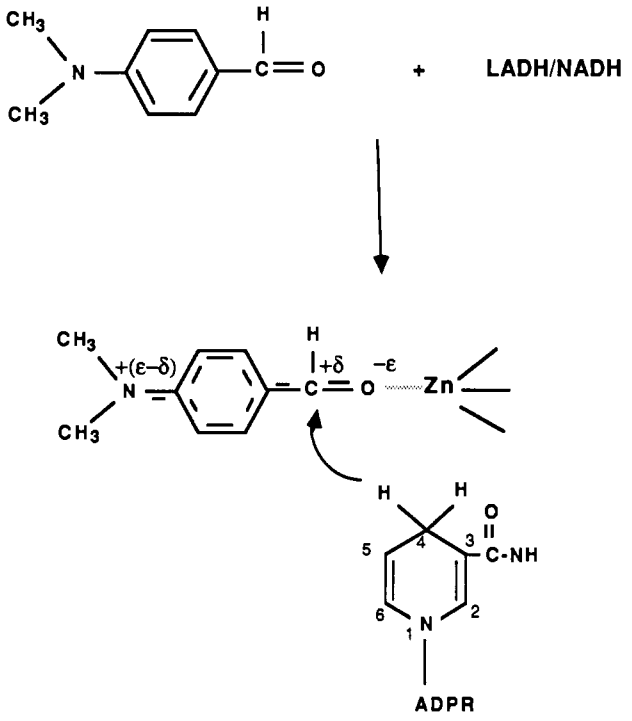

substrates should be of great utility in quantitatively relating the kinetic properties of each substrate to its molecular electronic properties in situ.

References

Angelis, C. T., Dunn, M. F., Muchmore, D. C., & Wing, R. M. (1977) *Biochemistry 16*, 2922–2931.

Biellmann, J.-F., & Jung, M. J. (1971) *Eur. J. Biochem. 19*, 130–134.

Blackmann, L. F., & Hardman, M. J. (1975) *Eur. J. Biochem. 55*, 611–615.

Brändén, C.-I., & Eklund, H. (1978) *Ciba Found. Symp. 60*, 63–80.

Brändén, C.-I., & Eklund, H. (1980) *Dehydrogenases Requiring Nicotinamide Coenzymes* (Jeffrey, J., Ed.) pp 441–484, Birkhaeuser Verlag, Basel.

Brändén, C.-I., Jornvall, H., Eklund, H., & Furugren, B. (1975) *Enzymes (3rd Ed.)* 103–190.

Carey, P. R., & Storer, A. C. (1984) *Annu. Rev. Biophys. Bioeng. 13*, 25–49.

Cedergren-Zeppezauer, E., Samama, J.-P., & Eklund, H. (1982) *Biochemistry 21*, 4895–4908.

Chen, D., Yue, K. T., Martin, C., Rhee, K. W., Sloan, D. L., & Callender, R. (1987) *Biochemistry 26*, 4776–4784.

Creighton, D. J., & Sigman, D. S. (1971) *J. Am. Chem. Soc. 93*, 6314–6316.

Dahl, K. H., & Dunn, M. F. (1984) *Biochemistry 23*, 4094–4100.

Dalziel, K. (1963) *J. Biol. Chem. 238*, 2850–2858.

de Groot, J. A., Gorter-La Roy, G. M., van Koeveringe, J. A., & Lugtenburg, J. (1981) *Org. Prep. Proced. Int. 13(2)*, 97–101.

Drysdale, B.-E., & Hollis, D. P. (1980) *Arch. Biochem. Biophys. 205*, 267–279.

Dunn, M. F., & Hutchison, J. S. (1973) *Biochemistry 12*, 4882–4892.

Dunn, M. F., Biellmann, J.-F., & Branlant, G. (1975) *Biochemistry 14*, 3176–3182.

Dworschack, R. T., & Plapp, B. V. (1977) *Biochemistry 16*, 2716–2725.

Eklund, H., & Brändén, C.-I. (1986) in *Pyridine Nucleotides*, Wiley, New York.

Eklund, H., Samama, J.-P., Wallen, L., Brändén, C.-I., Åkeson, Å., & Jones, T. A. (1981) *J. Mol. Biol. 146*, 561–587.

Fetizon, M., Henry, Y., Moreau, N., Moreau, G., Golfier, M., & Prange, T. (1973) *Tetrahedron 29*, 1011–1014.

Hartman, M. J., Blackwell, L. F., Boswell, C. R., & Buckley, P. D. (1974) *Eur. J. Biochem. 50*, 113–118.

Hertzberg, G. (1950) *Spectra of Diatomic Molecules*, 2nd ed., Van Nostrand Reinhold, New York.

Jagodzinski, P. W., & Peticolas, W. L. (1981) *J. Am. Chem. Soc. 103*, 234–236.

Jagodzinski, P. W., Funk, G. F., & Peticolas, W. L. (1982) *Biochemistry 21*, 2193–2202.

Kvassman, J., & Pettersson, G. (1978) *Eur. J. Biochem. 87*, 417–427.

Kvassman, J., & Pettersson, G. (1980a) *Eur. J. Biochem. 103*, 557–564.

Kvassman, J., & Pettersson, G. (1980b) *Eur. J. Biochem. 103*, 565–575.

MacGibbon, A. K. H., Koerber, S. C., Pease, K., & Dunn, M. F. (1987) *Biochemistry 26*, 3058–3067.

Morris, R. G., Saliman, G., & Dunn, M. F. (1980) *Biochemistry 19*, 725–731.

Pardoen, J. A., Winkel, C., Mulder, P. P. J., & Lugtenburg, J. (1984) *Recl. Trav. Chim. Pays-Bas 103*, 135–141.

Plapp, B. V., Eklund, H., & Brändén, C.-I. (1978) *J. Mol. Biol. 122*, 23–32.

Sasaki, Y., & Sugiura, M. (1974) *Chem. Pharm. Bull. 22*, 224–229.

Shore, J. D., Gutfreund, H., Brooks, R. L., Santiago, D., & Santiago, P. (1974) *Biochemistry 13*, 4185–4191.

Sloan, D. L., Young, J. M., & Mildvan, A. S. (1975) *Biochemistry 14*, 1998–2008.

Taniguchi, S., Theorell, H., & Åkeson, Å. (1967) *Acta Chem. Scand. 21*, 1903–1920.

Theorell, H., & Chance, B. (1951) *Acta Chem. Scand. 5*, 1127–1144.

Theorell, H., & McKinley-McKee, J. S. (1961) *Acta Chem. Scand. 15*, 1811–1833.

Yue, K. T., Yang, J.-P., Martin, C. L., Lee, S. K., Sloan, D. L., & Callender, R. H. (1984) *Biochemistry 23*, 6480–6483.